

Full length article

Performance analysis of Hexagonal QAM constellations on quadrature spatial modulation with perfect and imperfect channel estimation

Fatih Cogen^{a,b}, Erdogan Aydin^{b,*}^a Turkish–German University, Department of Mechatronics Engineering, Istanbul, Turkey^b Istanbul Medeniyet University, Department of Electrical and Electronics Engineering, Istanbul, Turkey

ARTICLE INFO

Article history:

Received 14 June 2020

Received in revised form 25 April 2021

Accepted 19 May 2021

Available online 29 May 2021

Keywords:

Spatial modulation

Quadrature spatial modulation

Hexagonal quadrature amplitude modulation

MIMO systems

ABSTRACT

In this study, the quadrature spatial modulation (QSM) technique, which is a rational multiple-input multiple-output (MIMO) transmission technique and frequently encountered in recent studies in the literature, and the hexagonal quadrature amplitude modulation (HQAM) constellation technique, which combines symbols in an “optimum” way are combined. This new MIMO scheme has been named by the authors as HQAM-QSM. Also, the impact of imperfect channel knowledge on the performance of the proposed scheme is examined. The HQAM constellation technique is a technique that provides better results under the same power assumption than the conventional QAM constellation in terms of symbol separation and is more often encountered when it comes to energy-efficiency. Due to the nature of HQAM symbols, error-floor occurs when the QSM system is applied. Hence, the optimum angle is obtained by rotating the HQAM symbols. With this optimum angle, it has been seen that the error-floor disappeared and the performance of the system is improved. Besides, the HQAM technique performs similar bit error rates (BER) to QAM at high signal-to-noise ratio (SNR) values. From this point forth, in our study, the rational HQAM-QSM technique, which uses energy-efficient HQAM symbols instead of traditional modulated QAM symbols and also carries information effectively on two active antennas, is proposed. Performance analysis of the HQAM-QSM technique is performed on Rayleigh fading channels.

© 2021 Elsevier B.V. All rights reserved.

1. Introduction

In today's world, communication technology is developing day by day, and the amount of energy usage increases with the growing service requirement accordingly. As a result, global greenhouse gas emissions are also rising in direct proportion. Another problem that is frequently encountered in our current lives is the battery shortage that everyone experiences. Unfortunately, the recent development of battery technology lags behind current communication technologies. For the reasons mentioned above, the concept of energy efficiency has become one of the most critical issues in next-generation communication systems [1,2].

Furthermore, many trends such as high-speed data transmission and reception, mobile and online gaming experience, high-definition (HD) video and audio broadcasting are increasing. Consequently, the requirements for high data rates, low latencies, high coverage, and high quality of service (QoS) in the next-generation of communication systems are increasing gradually. As predicted by experts, the number of devices connected

to the internet in 2020 will be more than 50 billion. From all those as mentioned above, it is an undeniable fact that the next-generation communication systems should be both fast, effective and energy-efficient [3].

Next-generation communication systems often use M -ary QAM (M -QAM) constellations because they are straightforward to implement and to be estimated. However, although this constellation structure is simple, one disadvantage of the M -QAM constellation is that it does not combine symbols well enough in terms of energy efficiency. Besides, M -QAM constellations cannot optimally separate each symbol from another under the same symbol energy assumption. In this context, M -QAM constellations are called sub-optimal according to the energy carried by the symbols. On the other hand, HQAM is an optimum two-dimensional constellation technique with a denser hexagonal lattice. The main aim of the HQAM technique is to minimize transmission power. [4–7] indicate that HQAM uses energy more effectively than conventional QAM constellations, makes a better separation between symbols under the same symbol power assumption, and has almost the same BER performance as QAM in higher SNR. A disadvantage of HQAM modulation is that it is complicated, but nowadays, especially with the development

* Corresponding author.

E-mail address: erdogan.aydin@medeniyet.edu.tr (E. Aydin).

of microprocessor technology in recent years, this is no longer a problem [8–12].

Multiple-input multiple-output (MIMO) communication systems, which have attracted considerable attention recently, have a prominent place among today's innovative communication techniques. MIMO communication systems play an essential role in increasing data rates and capacity. In MIMO systems, the receiver and transmitter are equipped with multiple antennas, the data stream is multiplexed on multiple transmitters on the transmitter side, and these signals are reassembled on the receiver side. This rational scheme provides a higher quality detection result than single-input and single-output (SISO) systems. Besides, the data rate increases considerably with the logical structures spatial modulation (SM), quadrature spatial modulation (QSM), and space-time block code (STBC), which cannot be found in SISO systems. SM is a rational MIMO technique that uses multi-transmit antennas as an extra dimension for data transmission. In SM technique, antennas are considered as spatial constellation points in addition to the conventional modulated symbols and increase the overall spectral efficiency. Each antenna index is used to carry additional information bits, and a spatial multiplexing gain of base-two logarithms of the total transmitting antennas is obtained. Besides, only one antenna is activated at a time in the SM technique. With this rational scheme, the inter-channel interference (ICI) is eliminated, inter-antenna synchronization is simplified, the receiver complexity is reduced, and only one RF chain is used in the transmitter. Despite all these advantages, one of SM's major criticisms is that the data rate is proportional to the base-two logarithms of the transmitting antennas, the data rate does not increase linearly [13–15]. From this point forth, HQAM based SM (HQAM-SM) technique was proposed by the authors in [16] for high data-rate and energy-efficient next-generation wireless communication systems. This proposed novel scheme is better in terms of energy-efficiency compared to traditional SM technique due to the nature of HQAM and is also more advantageous in terms of symbol separation at lower energies. In addition, the performance of HQAM-SM technique in Nakagami- m fading channels was also investigated in [17].

QSM is another MIMO technique that inherits almost all the advantages of SM and further enhances overall spectral efficiency. In QSM, the spatial constellation is divided into in-phase (I) and quadrature (Q) components, where the real part of the symbol is transmitted in the I component while the imaginary part in the Q component. In the QSM structure, two antennas are active at the same time, giving the SM a new dimension with the I and Q components. Since the I and Q components are orthogonal to each other, the signals do not interfere, and the ICI is completely avoided in the QSM as inherited from the SM. In other words, a portion of the signal is transmitted in the cosine carrier while another part is transmitted in the sine carrier. In the QSM scheme, since there are I and Q components, the spatial multiplexing gain is two-fold higher than SM [2,18].

Against this background, to the best of our knowledge, no work regarding the combination of HQAM constellation and QSM technique is available in the literature. In this study, a new scheme called HQAM-QSM is proposed, which will provide improvements to the QSM method in terms of energy efficiency. The main contributions of this paper are presented as follows:

1. By combining the HQAM and QSM techniques, a new and high data rated communication technique has been proposed and compared with well-known communication techniques such as QSM, SM, and M -QAM.
2. The impact of imperfect channel knowledge on the performance of the proposed scheme is examined.

3. The proposed new scheme takes advantage of the energy-efficient structure of the hexagonal constellation while providing an error rate similar to the QAM constellation at high SNR values in the QSM system.
4. Unlike QAM constellations, when the HQAM constellations are examined, it can easily be seen that the real and/or imaginary part of many symbols is zero. In the QSM system, if these symbols are used directly, it is not possible to obtain the bits carried in the antenna indices in which the zero components are transmitted. In such a case, the error-floor occurs. It has been proposed by the authors that HQAM symbols should be rotated to find the optimum angle in the QSM system to solve this situation. Besides, the optimum angle values of various HQAM constellations have been found, and these values have been confirmed by the simulation results.
5. The average bit error probability (ABEP) of the proposed HQAM-QSM scheme is derived based on the union bound technique.

The rest of this paper is organized as below. Section 2 describes the details of the HQAM-QSM scheme and HQAM constellation. Then, the theoretical analysis of the HQAM-QSM technique is performed in Section 3, and the simulation results and discussion are given in Section 4. Finally, Section 5 concludes this paper.

2. HQAM-QSM system model

In this section, the proposed HQAM-QSM scheme will be analyzed in two parts: Hexagonal QAM technique and Quadrature Spatial Modulation technique.

2.1. Hexagonal QAM constellation

The representation of hexagonal constellations for different values of $M = 4, 8, 16, 32, 64,$ and 128 is given in Fig. 1. As can be seen from this figure, HQAM constellations can minimize the transmitted power in the context of symbol separation and offer potential solutions to the energy-efficiency problem.

In the past, optimum hexagonal constellations were less favored than traditional QAM constellations. This was mainly due to the complexity of the hexagonal constellations at the point of symbol generation and decision-making at the receiver. However, this problem has ceased to exist due to the development of computer science and microprocessor technology. Due to its importance, we emphasize again that the main reason for this interest in hexagonal constellations is that, unlike the traditional QAM constellations, the hexagonal constellation is arranged “optimally” not “sub-optimally” [5].

To determine the hexagonal constellation points, the M -ary optimum hexagonal constellation points are formed by selecting the lowest powered M points starting from a given starting point. The hexagonal constellation with $M = 7$ is presented in Fig. 2. The average of these points creates a new starting point, and using this point; the new lowest powered M point is selected. This algorithm is continued in this way, and if the minimum distance between each point in a constellation and the other points decreases to zero, the process is terminated, and optimum constellations are formed. Otherwise, the process proceeds as described above [5].

Hexagonal constellation points are usually parameterized by two integers, such as i and j . Assuming that points a and b represent the k th constellation point, the hexagonal constellation point can be expressed as follows [19]:

$$(a_k, b_k) = \sqrt{\rho} \left((a_0, b_0) + i_k(1, 0) + j_k \left(\frac{1}{2}, \frac{\sqrt{3}}{2} \right) \right), \quad (1)$$

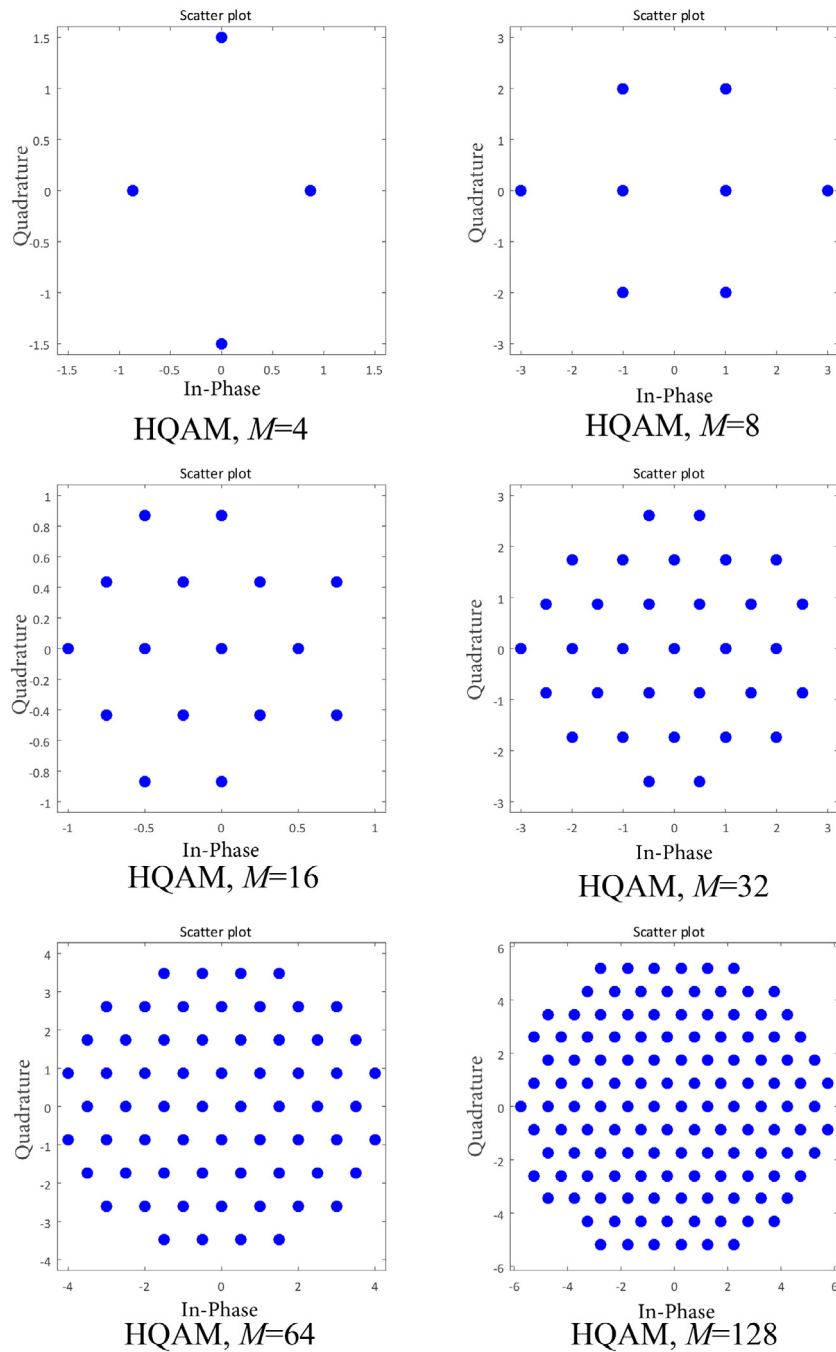


Fig. 1. Hexagonal constellations for $M = 4, 8, 16, 64$ and $M = 128$.

where, $\sqrt{\rho}$ can be expressed as the minimum distance ($d_{min} = \sqrt{\rho}$) between adjacent constellation points. The expression (a_0, b_0) is selected in such a way as to minimize the maximum energy. It should be noted that if hexagonal coordinates are subjected to the orthogonal rotation, there is absolutely no change in their properties. Besides, the average energy E_{avg} in terms of the above expressions and the maximum energy E_{max} can be given as follows [19]:

$$E_{avg} \triangleq \frac{\rho}{M} \sum_{k=1}^M \left\| \left((a_0 + i_k + \frac{j_k}{2}), (b_0 + j_k \frac{\sqrt{3}}{2}) \right) \right\|^2, \quad (2)$$

$$E_{max} \triangleq \rho \max_k \left\| \left((a_0 + i_k + \frac{j_k}{2}), (b_0 + j_k \frac{\sqrt{3}}{2}) \right) \right\|^2. \quad (3)$$

where $k = 1, 2, \dots, M$.

From this point on, the average power and constellation figure of merit (CFM) expressions will be defined to explain the benefits of HQAM better. Furthermore, by using these expressions, the energy-efficiency of HQAM will be better explained by comparing various HQAM constellation schemes and conventional QAM constellations. In this context, to better understand the advantages of HQAM-QAM constellation, we find it appropriate to provide the following explanation:

1. Suppose that any point of a constellation is represented by complex number $\mathcal{A}_k = a + jb$. As it is well known from the communication theory, the power of this point is given as $|\mathcal{A}_k|^2 = a^2 + b^2$. Assuming that all symbols of the constellation are equally probable, the average transmitted

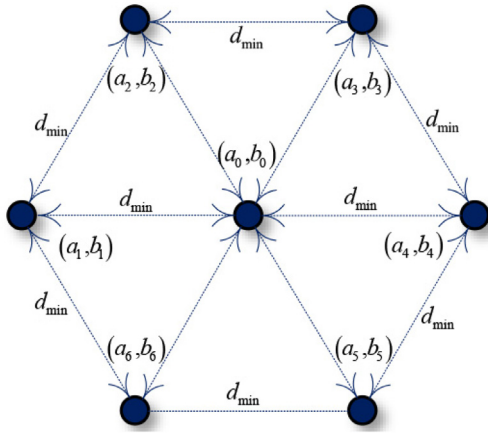


Fig. 2. Hexagonal constellation with $M = 7$.

Table 1
Average power and CFM values of hexagonal constellations for $M = 8$.

Constellation design	Average power (P_{avg})	CFM (ξ)
QAM	6	0.6667
SQAM	6	0.6667
HQAM	5	0.8
CQAM	4.6482	0.86055
DDQAM	1.1250	0.8889
HHQAM	1.1250	0.8889

signal power can be given as follows:

$$P_{avg} = \frac{1}{M} \sum_{k=1}^M |\mathcal{A}_k|^2. \quad (4)$$

- CFM is a scale used to measure the quality of any constellation used. If any constellation has a higher CFM than the other, it usually performs better. To be fair, the CFM expression should be used to compare the performance of constellations equal to the number of bits per dimension. It can also be said that CFM is a measure of how effectively constellation uses SNR. The CFM expression can be given as follows:

$$\xi = \frac{d_{min}^2}{P_{avg}}. \quad (5)$$

2.2. The energy efficiency analysis

In the considered HQAM-QSM communication technique, m_2 bits are transmitted over directly by the modulated HQAM symbol while m_1 bits are conveyed through the active antenna indices of QSM scheme. Hence, transmission energy of m_1 bits are not directly consumed by the HQAM-QSM scheme but it is carried with the active antenna indices of QSM system. As a result, according to the HQAM-QSM scheme, the percentage of energy-saving (\mathcal{E}_{sav}) per $m_{HQAM-QSM}$ bits can be written as follows:

$$\mathcal{E}_{sav} = \left(1 - \frac{m_2}{m_{HQAM-QSM}}\right) E_b\%, \quad (6)$$

here E_b is the bit energy, which is expressed as $\frac{E_s}{m_{HQAM-QSM}}$, where E_s is the symbol energy. Considering Table 1, the average power of the traditional QAM symbols for the same M value is higher than the average power of the HQAM symbols. For example, $E_{s,QAM} = 1.2E_{s,HQAM}$ and $E_{s,QAM} = 1.17E_{s,HQAM}$ when $M = 64, 256, 1024$ and $M = 128, 512$, respectively [16]. Therefore, the HQAM

Table 2
Energy-saving (\mathcal{E}_{sav}) comparisons of HQAM-QSM scheme in percentage compared to HQAM and QAM systems.

m_1	m_2	HQAM	QAM
2	6	25%	30%
4	6	40%	48%
6	6	50%	60%
8	6	57.14%	68.57%
8	7	53.33%	62.4%
8	8	50%	60%

Table 3
The optimum rotation angle values for the various HQAM constellations.

Constellation type	Optimum angle (ϕ_{opt})
HQAM-QSM, $M = 4$	45°
TQAM-QSM, $M = 4$	75°
HQAM-QSM, $M = 8$	45°
TQAM-QSM, $M = 8$	86.11°
DDQAM-QSM, $M = 8$	27.93°
TQAM-QSM, $M = 16$	1.54°
TQAM-QSM, $M = 32$	88.64°
TQAM-QSM, $M = 64$	90°
TQAM-QSM, $M = 128$	90°

technique has the percentage of energy-saving 16.3% and 13.8% $M = 64, 256, 1024$ and $M = 128, 512$, respectively, according to the QAM technique. In Table 2, energy-saving comparisons of HQAM-QSM scheme in percentage compared to HQAM and QAM schemes for various m_1 and m_2 bits values are given. For instance, when the number of bits transmitted is selected as $m_{HQAM-QSM} = 15$ ($m_1 = 8, m_2 = 7$) the \mathcal{E}_{sav} of the HQAM-QSM system compared to the HQAM and QAM technique is 53.33% and 62.4%, respectively. Considering Table 2, it is seen that the HQAM-QSM system is reasonably energy efficiency scheme compared to HQAM and QAM systems.

To better understand these concepts, the P_{avg} and ξ expressions will be calculated over the 8-ary constellation schemes given in Fig. 3 and Table 1. As can be seen from Table 1 above, when the case is examined for simple QAM schemes, HQAM, Circle (7,1) (CQAM), Hexagonal Double Diamond (DDQAM), and Hexagonal Heart (HHQAM) constellation schemes provide 16.67%, 22.53%, 81.25%, and 81.25% respectively compared to traditional QAM and Square QAM (SQAM) constellations. Among these constellations, it would be wise to use DDQAM and HHQAM schemes because they have both high energy-efficiency and have high CFM values [20–22].

2.3. Optimization of HQAM constellation for QSM

Algorithm 1: HQAM-QSM Optimal Angle Detection Algorithm.

Inputs:

Specify the constellation type
 M , specify the modulation order.
 Create an array **angle_iteration**
 Create a matrix **constellation**
constellation ← constellation symbols
angle_iteration ← 0° to 360°
 $i \leftarrow 0$

while **angle_iteration**(i) \neq NULL **do**
 new_constellation ← rotate(**constellation**, i)
 BER_value(i) ← BER_calculation(**new_constellation**)
 $i = i + 1$

end

$\phi_{opt} \leftarrow \text{min_index}(\text{BER_value})$

return ϕ_{opt}

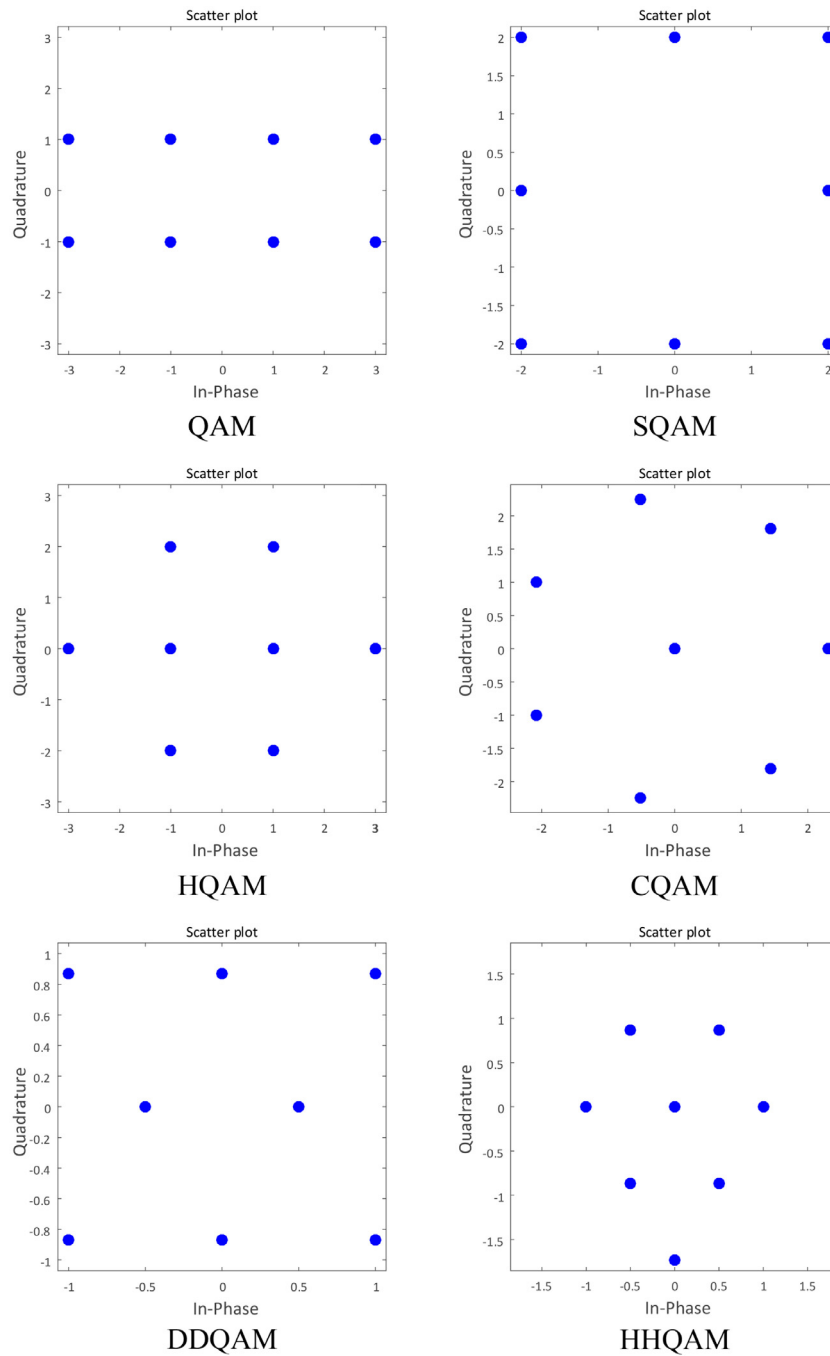


Fig. 3. Hexagonal constellations for $M = 8$.

In this subsection, it will be explained in detail how to find the optimum rotation angle values of the HQAM symbols used in the HQAM-QSM system to further improve the error performance of the proposed system. The main factor affecting the performance of the system is whether the HQAM constellation contains the $x = 0$ symbol. If the HQAM constellation contains the $x = 0$ symbol, the bits carried in the indices cannot be obtained correctly in the receiver and therefore the index error will always be 0.5.¹ Also, in the case of $x \neq 0$, the performance of the proposed system can be further improved by rotating the constellation to obtain the optimum angle.²

2.3.1. If HQAM constellation do not contain $x = 0$ symbol

As stated before, it has been suggested by the authors that the use of HQAM symbols in the QSM system by rotating will provide benefits in the context of BER performance. Also, the rotation angles that provide the optimum performance by rotating various HQAM constellations individually have been found by considering Algorithm 1 and also the optimum angle values of the various HQAM constellations used in this study are given in Table 3. For example, when the modulation degree of the HQAM constellation is $M = 4, 8$, the optimum angles are 45° and 75° , respectively. Besides, in the “Simulation Results and Discussion” section, the effects of rotation angles on performance have been examined in detail through computer simulations based on Algorithm 1.

¹ This situation is discussed in Section 2.3.2.

² This situation is discussed in Section 2.3.1.

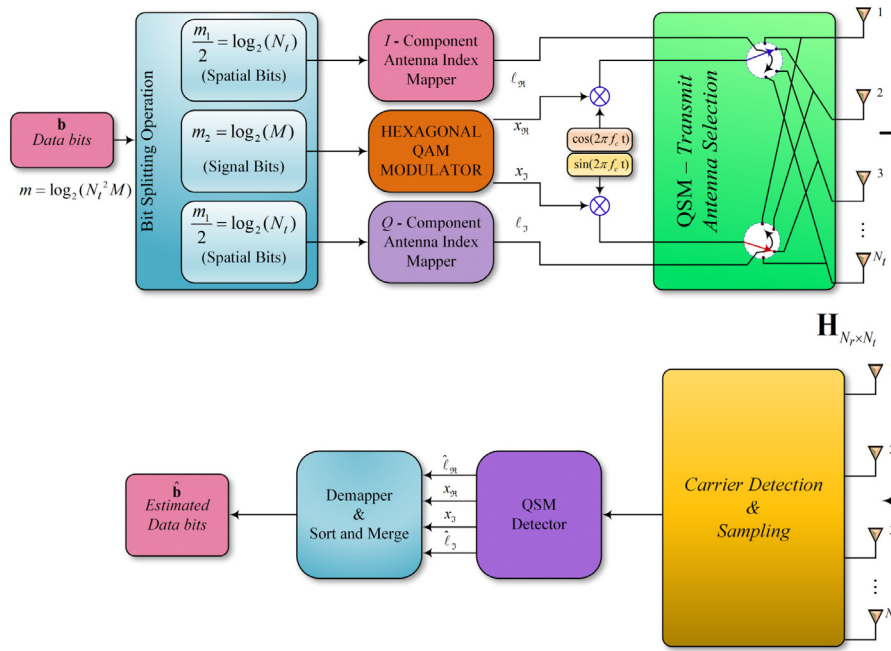


Fig. 4. HQAM-QSM system model.

2.3.2. If HQAM constellation contains $x = 0$ symbol ($x_{\Re} = 0, x_{\Im} = 0$)

As it is known, the classical QSM system sends the real part of the symbol from one transmit antenna while the imaginary part from another transmit antenna. However, unlike classical QAM constellation, in many cases of HQAM constellation, the amplitude of the symbol's real or imaginary parts appears to be close to zero or zero. In this case, as the real or imaginary part of the symbols in the QSM structure is multiplied by the channel of the active transmit antenna and sent to the receiver terminal. Thus, the receiver loses channel information (consequently antenna indices information), and error-floor occurs in the performance of the HQAM-QSM. The ways to correct this unwanted situation are as follows:

- Step 1 Use hexagonal constellation schemes with symbols without zero amplitude. In particular, Triangular QAM (TQAM) constellations can be very helpful in this regard because by nature, no scheme of TQAM contains (0,0) point, so for all of the constellation's points $x_{\Re} \neq 0, x_{\Im} \neq 0$. Here, x_{\Re} and x_{\Im} are the real and imaginary components of modulated symbol of $x = x_{\Re} + jx_{\Im}$. Besides, the constellation points are positioned to form an equilateral triangle. However, it should be noted that not every TQAM scheme provides the best performance. In some cases of TQAM (such as $M = 4, 8$), the rotation angle method proposed in Step 2 should be used.
- Step 2 Rotate hexagonal constellation schemes with a real or imaginary component are zero until you reach the optimum angle (ϕ_{opt}) to maximize system performance. However, the constellation point of (0,0) is not affected by rotation. As a result, even if the constellation schemes containing the point (0,0), i.e $x = 0$ are subjected to the rotation, they will reduce the performance of the system and error-floor will occur.
- Step 3 Shifting the constellations that contain (0,0) is another solution, but this method steals from HQAM's optimum energy criterion, which we do not want. However, it may be necessary to do this in cases such as HQAM with $M = 16$ that contain (0,0) point.

The above conditions will be explained in detail in the simulation results section.

2.4. HQAM-QSM transmission model and ML detector

The system model of the proposed HQAM-QSM system is shown in Fig. 4. The HQAM-QSM system consists of N_t transmitting antennas and N_r receiving antennas. As it is known, in the QSM system, similar to the SM system, antennas carry data in addition to the conventional symbols, and since this data transmission is done via orthogonal I and Q channels, the data-rate increases automatically and ICI is eliminated. Besides, in the proposed system, the QSM technique uses an energy-efficient HQAM constellation scheme as opposed to conventional constellation schemes.

When the system model of the HQAM system is examined, it is seen that the \mathbf{b} vector with the size of $1 \times m$ is the information vector to be transmitted by the transmitter. In the transmitter terminal, this information vector \mathbf{b} is divided into $m_1 = \log_2(N_t^2)$ and $m_2 = \log_2(M)$ bit long sub-information vectors, where $m = m_1 + m_2$ and the information transmission is carried out by means of these sub-vectors. The signal constellation symbol x is then divided into the sub-components x_{\Re} and x_{\Im} so that $x = x_{\Re} + jx_{\Im}$ and processed by a single IQ-RF chain:

$$s = \Re[xe^{-j2\pi f_c t}] = x_{\Re} \cos(2\pi f_c t) + x_{\Im} \sin(2\pi f_c t). \quad (7)$$

As seen from (7), x_{\Re} is transmitted over the cosine carrier, and x_{\Im} is transmitted over the sine carrier. In the QSM system, additional bits of $\log_2(N_t)$ are sent from both the I and Q channels, unlike the SM system, so that the real part of the bits is I and the imaginary part is sent in the Q component. As stated previously, the I and Q channels are orthogonal to each other, and the ICI is completely prevented on the receiver side. Let us try to explain the structure of HQAM-QSM with an example and assume that we use a simple QAM constellation with $M = 4$ instead of using HQAM to make the explanation simpler. Suppose that the data series $m = [1 \ 0 \ 0 \ 1 \ 1 \ 0]$ will be transmitted by the transmitter

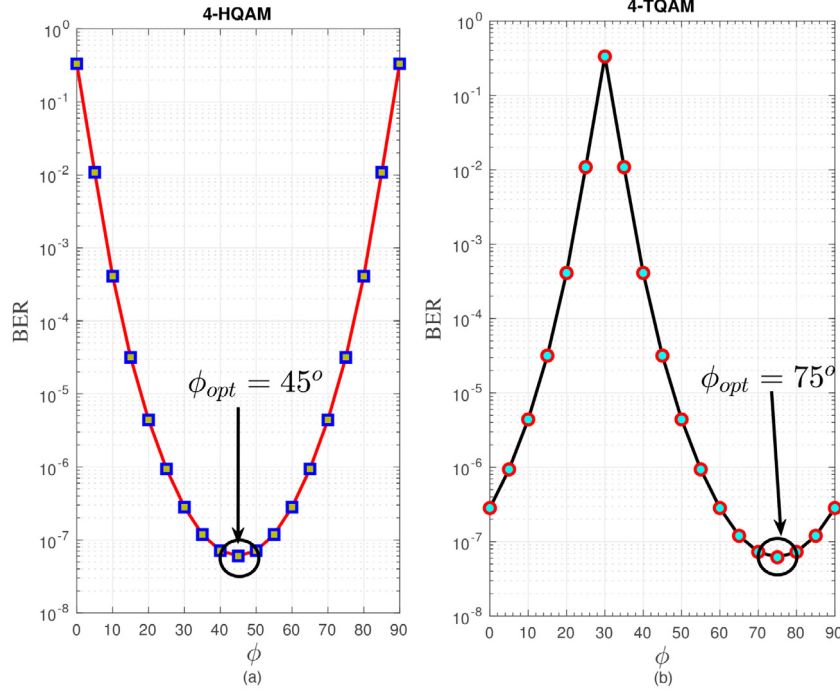


Fig. 5. BER vs. rotation angle of HQAM-QSM and TQAM-QSM scheme when $M = 4$ and SNR of 15 dB .

using $N_t = 4$ transmission antennas. The first $\log_2(M)$ bits $[1\ 0]$ modulates the 4-QAM symbol, where $x = 1 - j$. This symbol is then divided into $x_{\Re} = +1$ and $x_{\Im} = -1$ to be sent its real part from the I and the imaginary part from the Q component. The second $\log_2(N_t)$ bits $[0\ 1]$ modulates the first active antenna index and selects the active antenna index $\ell_{\Re} = 2$ and sends the $x_{\Re} = +1$. Here, the resulting transmitted real vector becomes $\mathbf{s}_{\Re} = [0\ 1\ 0\ 0]^T$. The last $\log_2(N_t)$ bit $[1\ 0]$ modulates the second active antenna index and selects the $\ell_{\Im} = 3$ active antenna index and sends the $x_{\Im} = -1$. Here, the resulting transmitted imaginary vector becomes $\mathbf{s}_{\Im} = [0\ 0\ -1\ 0]^T$. The transmitted vector is given as the sum of real and imaginary vectors as follows: $\mathbf{s} = \mathbf{s}_{\Re} + j\mathbf{s}_{\Im} = [0\ -1\ -j\ 0]^T$.

The noisy and faded HQAM-QSM signal coming to the receiver can be given as follows:

$$\begin{aligned} \mathbf{r} &= \sqrt{E_s}\mathbf{H}\mathbf{s} + \mathbf{n}, \\ &= \sqrt{E_s}\mathbf{H}(\mathbf{s}_{\Re} + j\mathbf{s}_{\Im}) + \mathbf{n}, \\ &= \sqrt{E_s}(\mathbf{h}_{\ell_{\Re}}x_{\Re} + j\mathbf{h}_{\ell_{\Im}}x_{\Im}) + \mathbf{n}, \quad \ell_{\Re}, \ell_{\Im} \in \{1, \dots, N_t\}, \end{aligned} \quad (8)$$

where E_s is the symbol energy, x is the HQAM symbol, the $h_{i,j}$ -th element of the matrix \mathbf{H} defines the channel gain between the i th transmitting antenna and the j th receiver antenna, and $\mathbf{h}_{\ell_{\Re}}$ and $\mathbf{h}_{\ell_{\Im}}$ are the ℓ_{\Re} -th ve ℓ_{\Im} -th columns of the matrix \mathbf{H} , respectively. That is, $\mathbf{h}_{\ell_{\Re}} = [h_{1,\ell_{\Re}}, h_{2,\ell_{\Re}}, \dots, h_{N_r,\ell_{\Re}}]^T$ and $\mathbf{h}_{\ell_{\Im}} = [h_{1,\ell_{\Im}}, h_{2,\ell_{\Im}}, \dots, h_{N_r,\ell_{\Im}}]^T$ where $\mathbf{h}_{\ell_{\Re}}$ and $\mathbf{h}_{\ell_{\Im}} \sim \mathcal{CN}(0, \sigma_h^2 = 1)$, \mathbf{n} is the complex variable gauss random variable with N_r dimension, and its variance is N_0 , that is $\mathcal{CN}(0, N_0)$.

Under the assumption that the receiver has excellent channel information, the Maximum Likelihood (ML) decoder for the HQAM-QSM system can be given as follows:

$$\begin{aligned} [\hat{\ell}_{\Re}, \hat{\ell}_{\Im}, \hat{x}_{\Re}, \hat{x}_{\Im}] &= \arg \min_{\ell_{\Re}, \ell_{\Im}, x_{\Re}, x_{\Im}} \left\| \mathbf{r} - \sqrt{E_s}\mathbf{H}\mathbf{s} \right\|^2 \\ &= \arg \min_{\ell_{\Re}, \ell_{\Im}, x_{\Re}, x_{\Im}} \left\| \mathbf{r} - \sqrt{E_s}(\mathbf{h}_{\ell_{\Re}}x_{\Re} + j\mathbf{h}_{\ell_{\Im}}x_{\Im}) \right\|^2 \end{aligned}$$

$$= \arg \min_{\ell_{\Re}, \ell_{\Im}, x_{\Re}, x_{\Im}} \left\{ \|\mathbf{a}\|^2 - 2\Re\{\mathbf{r}^H\mathbf{a}\} \right\}. \quad (9)$$

Here, $(\cdot)^H$ defines the Hermitian of a vector, $\|\cdot\|$ defines the norm, and $\mathbf{a} = \sqrt{E_s}(\mathbf{h}_{\ell_{\Re}}x_{\Re} + j\mathbf{h}_{\ell_{\Im}}x_{\Im})$. Finally, the detected antenna indices $(\hat{\ell}_{\Re}, \hat{\ell}_{\Im})$ and the data symbols $(\hat{x}_{\Re}, \hat{x}_{\Im})$ are used to recover the original information bits.

2.5. Impact of imperfect channel knowledge on HQAM-QSM technique

In this section, the effect of the channel estimation error on the HQAM-QSM system in the absence of perfect CSI in the receiver will be presented. Assuming that there is a orthogonality between the estimation of the channel coefficients and the estimation error, the expression $h_{i,j}$ can be given as follows [23]:

$$h_{i,j} = \hat{h}_{i,j} + \epsilon_{h_{i,j}}, \quad (10)$$

where \hat{h} represents the estimation of channel coefficients. \hat{h} and $h_{i,j}$ are assumed to have a jointly ergodic and stationary Gaussian process. $\epsilon_{h_{i,j}}$ is defined as channel estimation error and is modeled as complex Gaussian variable with zero mean and σ_ϵ^2 variance, i.e., $\mathcal{CN}(0, \sigma_\epsilon^2)$. In this model, σ_ϵ^2 is used to show the change in channel estimation performance and can be defined differently according to the channel estimation methods and the channel dynamics. Assuming that orthogonal pilot channel estimation symbols are used, the estimation error decreases linearly by increasing the number of pilot symbols.

In the case of imperfect channel knowledge, the ML detector in (9) can be rewritten for HQAM-QSM system as follows:

$$\begin{aligned} [\hat{\ell}_{\Re}, \hat{\ell}_{\Im}, \hat{x}_{\Re}, \hat{x}_{\Im}] &= \arg \min_{\ell_{\Re}, \ell_{\Im}, x_{\Re}, x_{\Im}} \left\| \mathbf{r} - \sqrt{E_s}\hat{\mathbf{H}}\mathbf{s} \right\|^2 \\ &= \arg \min_{\ell_{\Re}, \ell_{\Im}, x_{\Re}, x_{\Im}} \left\| \mathbf{r} - \sqrt{E_s}(\hat{\mathbf{h}}_{\ell_{\Re}}x_{\Re} + j\hat{\mathbf{h}}_{\ell_{\Im}}x_{\Im}) \right\|^2 \\ &= \arg \min_{\ell_{\Re}, \ell_{\Im}, x_{\Re}, x_{\Im}} \left\{ \|\tilde{\mathbf{a}}\|^2 - 2\Re\{\mathbf{r}^H\tilde{\mathbf{a}}\} \right\}. \end{aligned} \quad (11)$$

where, $\hat{\mathbf{a}} = \sqrt{E_s}(\hat{\mathbf{h}}_{\ell_{3\mathcal{R}}}x_{3\mathcal{R}} + j\hat{\mathbf{h}}_{\ell_{3\mathcal{I}}}x_{3\mathcal{I}})$. $\hat{\mathbf{h}}_{\ell_{3\mathcal{R}}}$ and $\hat{\mathbf{h}}_{\ell_{3\mathcal{I}}}$ are the $\ell_{3\mathcal{R}}$ -th and $\ell_{3\mathcal{I}}$ -th columns of the matrix $\hat{\mathbf{H}}$, respectively. That is, $\hat{\mathbf{h}}_{\ell_{3\mathcal{R}}} = [\hat{h}_{1,\ell_{3\mathcal{R}}}, \hat{h}_{2,\ell_{3\mathcal{R}}}, \dots, \hat{h}_{N_r,\ell_{3\mathcal{R}}}]^T$ and $\hat{\mathbf{h}}_{\ell_{3\mathcal{I}}} = [\hat{h}_{1,\ell_{3\mathcal{I}}}, \hat{h}_{2,\ell_{3\mathcal{I}}}, \dots, \hat{h}_{N_r,\ell_{3\mathcal{I}}}]^T$.

3. Performance analysis

In this section, we evaluate the error performance of the HQAM-QSM system. The average bit error probability (ABEP) \mathcal{P}_e can be expressed using the asymptotically tight union bound as [24]:

$$\mathcal{P}_e \approx \frac{1}{2^m} \sum_{i=1}^{2^m} \sum_{j=1}^{2^m} \frac{1}{m} \mathcal{P}_e(\mathbf{a}_i \rightarrow \hat{\mathbf{a}}_j) e_{i,j}, \quad (12)$$

where $m = \log_2(N_s^2 M)$ is the number of bits transmitted in the active antenna indices and the modulated symbol, $e_{i,j}$ is defined as the number of bit errors associated with the corresponding pairwise error event, and $\mathcal{P}_e(\mathbf{a}_i \rightarrow \hat{\mathbf{a}}_j)$ is the average pairwise error probability (APEP), where $\mathbf{a}_i = \sqrt{E_s}(\mathbf{h}_{\ell_{3\mathcal{R}}}x_{3\mathcal{R}} + j\mathbf{h}_{\ell_{3\mathcal{I}}}x_{3\mathcal{I}})$ and $\hat{\mathbf{a}}_j = \sqrt{E_s}(\hat{\mathbf{h}}_{\ell_{3\mathcal{R}}}\hat{x}_{3\mathcal{R}} + j\hat{\mathbf{h}}_{\ell_{3\mathcal{I}}}\hat{x}_{3\mathcal{I}})$, $\hat{\mathbf{s}}$ is a pairwise of \mathbf{s} .

The conditional PEP (CPEP) of the HQAM-QSM system is calculated as follows [24]:

$$\begin{aligned} \mathcal{P}(\mathbf{a}_i \rightarrow \hat{\mathbf{a}}_j | \mathbf{H}) &= \mathcal{P}\left(\|\mathbf{r} - \sqrt{E_s}\mathbf{H}\mathbf{s}\|^2 > \|\mathbf{r} - \sqrt{E_s}\mathbf{H}\hat{\mathbf{s}}\|^2\right) \\ &= Q\left(\sqrt{\frac{\|\mathbf{H}(\mathbf{a}_i - \hat{\mathbf{a}}_j)\|^2}{2N_0}}\right), \end{aligned} \quad (13)$$

where $Q(y)$ is the Q-function, which can be written as $Q(y) = \frac{1}{\pi} \int_0^{\pi/2} e^{-y^2/2 \sin^2 \theta} d\theta$, and hence, CPEP can be expressed as:

$$\mathcal{P}(\mathbf{a}_i \rightarrow \hat{\mathbf{a}}_j | \mathbf{H}) = \frac{1}{\pi} \int_0^{\pi/2} \exp\left(-\frac{\|\mathbf{H}(\mathbf{a}_i - \hat{\mathbf{a}}_j)\|^2}{4N_0 \sin^2 \theta}\right) d\theta. \quad (14)$$

Then, unconditional PEP (UPEP) of the HQAM-QSM scheme is determined as follows by averaging (14) considering the moment generating function (MGF):

$$\mathcal{P}(\mathbf{a}_i \rightarrow \hat{\mathbf{a}}_j) = \frac{1}{\pi} \int_0^{\pi/2} \left(\frac{\sin^2 \theta}{\sin^2 \theta + \frac{\|\mathbf{a}_i - \hat{\mathbf{a}}_j\|^2}{4N_0}}\right)^{N_r} d\theta. \quad (15)$$

Finally, UPEP can be calculated as [24]:

$$\mathcal{P}_e(\mathbf{a}_i \rightarrow \hat{\mathbf{a}}_j) = \psi^{N_r} \sum_{j=0}^{N_r-1} \binom{N_r-1+j}{j} [1-\psi]^j, \quad (16)$$

where $\psi = \frac{1}{2} \left(1 - \sqrt{\frac{\bar{\kappa}/2}{1+\bar{\kappa}/2}}\right)$, and $\bar{\kappa}$ is the mean of the exponential random variable κ and can be expressed as [24]:

$$\bar{\kappa} = \begin{cases} \frac{E_s}{2N_0} \sigma_h^2 (|\mathcal{X}_{3\mathcal{R}}|^2 + |\hat{\mathcal{X}}_{3\mathcal{R}}|^2 + |\mathcal{X}_{3\mathcal{I}}|^2 + |\hat{\mathcal{X}}_{3\mathcal{I}}|^2) & \text{if } \mathbf{h}_{\ell_{3\mathcal{R}}} \neq \hat{\mathbf{h}}_{\ell_{3\mathcal{R}}}, \mathbf{h}_{\ell_{3\mathcal{I}}} \neq \hat{\mathbf{h}}_{\ell_{3\mathcal{I}}} \\ \frac{E_s}{2N_0} \sigma_h^2 (|\mathcal{X}_{3\mathcal{R}} - \hat{\mathcal{X}}_{3\mathcal{R}}|^2 + |\mathcal{X}_{3\mathcal{I}}|^2 + |\hat{\mathcal{X}}_{3\mathcal{I}}|^2) & \text{if } \mathbf{h}_{\ell_{3\mathcal{R}}} = \hat{\mathbf{h}}_{\ell_{3\mathcal{R}}}, \mathbf{h}_{\ell_{3\mathcal{I}}} \neq \hat{\mathbf{h}}_{\ell_{3\mathcal{I}}} \\ \frac{E_s}{2N_0} \sigma_h^2 (|\mathcal{X}_{3\mathcal{R}}|^2 + |\hat{\mathcal{X}}_{3\mathcal{R}}|^2 + |\mathcal{X}_{3\mathcal{I}} - \hat{\mathcal{X}}_{3\mathcal{I}}|^2) & \text{if } \mathbf{h}_{\ell_{3\mathcal{R}}} \neq \hat{\mathbf{h}}_{\ell_{3\mathcal{R}}}, \mathbf{h}_{\ell_{3\mathcal{I}}} = \hat{\mathbf{h}}_{\ell_{3\mathcal{I}}} \\ \frac{E_s}{2N_0} \sigma_h^2 (|\mathcal{X}_{3\mathcal{R}} - \hat{\mathcal{X}}_{3\mathcal{R}}|^2 + |\mathcal{X}_{3\mathcal{I}} - \hat{\mathcal{X}}_{3\mathcal{I}}|^2) & \text{if } \mathbf{h}_{\ell_{3\mathcal{R}}} = \hat{\mathbf{h}}_{\ell_{3\mathcal{R}}}, \mathbf{h}_{\ell_{3\mathcal{I}}} = \hat{\mathbf{h}}_{\ell_{3\mathcal{I}}} \end{cases} \quad (17)$$

The asymptotic mean PEP expression of the proposed system is obtained as follows if Eq. (16) is extended to the Taylor series,

and the high-grade terms are neglected:

$$\bar{\mathcal{P}}_e(\mathbf{a}_i \rightarrow \hat{\mathbf{a}}_j) = \frac{2^{N_r-1} \Gamma(N_r + 0.5)}{\sqrt{\pi} (N_r)!} \left(\frac{1}{\bar{\kappa}}\right)^{N_r}, \quad (18)$$

where $\Gamma(\cdot)$ is the gamma function.

Finally, substituting (16) and (17) into (12), we obtain the total probability of the error for HQAM-QSM scheme.

3.1. Impact of imperfect channel knowledge on performance analysis

Similar to the theoretical expressions for the case where perfect CSI is known at the receiver, in the case of imperfect channel knowledge, ABEP can also be expressed by (12). In this approach, only $\bar{\kappa}$ expression in (17) can be rewritten as follows [23]:

$$\bar{\kappa} = \begin{cases} \frac{E_s (\sigma_h^2 - \sigma_\epsilon^2)}{4N_0 + 2\sigma_\epsilon^2 E_s (|\mathcal{X}_{3\mathcal{R}}|^2 + |\mathcal{X}_{3\mathcal{I}}|^2)} (|\mathcal{X}_{3\mathcal{R}}|^2 + |\hat{\mathcal{X}}_{3\mathcal{R}}|^2 + |\mathcal{X}_{3\mathcal{I}}|^2 + |\hat{\mathcal{X}}_{3\mathcal{I}}|^2) & \text{if } \mathbf{h}_{\ell_{3\mathcal{R}}} \neq \hat{\mathbf{h}}_{\ell_{3\mathcal{R}}}, \mathbf{h}_{\ell_{3\mathcal{I}}} \neq \hat{\mathbf{h}}_{\ell_{3\mathcal{I}}} \\ \frac{E_s (\sigma_h^2 - \sigma_\epsilon^2)}{4N_0 + 2\sigma_\epsilon^2 E_s (|\mathcal{X}_{3\mathcal{R}}|^2 + |\mathcal{X}_{3\mathcal{I}}|^2)} (|\mathcal{X}_{3\mathcal{R}} - \hat{\mathcal{X}}_{3\mathcal{R}}|^2 + |\mathcal{X}_{3\mathcal{I}}|^2 + |\hat{\mathcal{X}}_{3\mathcal{I}}|^2) & \text{if } \mathbf{h}_{\ell_{3\mathcal{R}}} = \hat{\mathbf{h}}_{\ell_{3\mathcal{R}}}, \mathbf{h}_{\ell_{3\mathcal{I}}} \neq \hat{\mathbf{h}}_{\ell_{3\mathcal{I}}} \\ \frac{E_s (\sigma_h^2 - \sigma_\epsilon^2)}{4N_0 + 2\sigma_\epsilon^2 E_s (|\mathcal{X}_{3\mathcal{R}}|^2 + |\mathcal{X}_{3\mathcal{I}}|^2)} (|\mathcal{X}_{3\mathcal{R}}|^2 + |\hat{\mathcal{X}}_{3\mathcal{R}}|^2 + |\mathcal{X}_{3\mathcal{I}} - \hat{\mathcal{X}}_{3\mathcal{I}}|^2) & \text{if } \mathbf{h}_{\ell_{3\mathcal{R}}} \neq \hat{\mathbf{h}}_{\ell_{3\mathcal{R}}}, \mathbf{h}_{\ell_{3\mathcal{I}}} = \hat{\mathbf{h}}_{\ell_{3\mathcal{I}}} \\ \frac{E_s (\sigma_h^2 - \sigma_\epsilon^2)}{4N_0 + 2\sigma_\epsilon^2 E_s (|\mathcal{X}_{3\mathcal{R}}|^2 + |\mathcal{X}_{3\mathcal{I}}|^2)} (|\mathcal{X}_{3\mathcal{R}} - \hat{\mathcal{X}}_{3\mathcal{R}}|^2 + |\mathcal{X}_{3\mathcal{I}} - \hat{\mathcal{X}}_{3\mathcal{I}}|^2) & \text{if } \mathbf{h}_{\ell_{3\mathcal{R}}} = \hat{\mathbf{h}}_{\ell_{3\mathcal{R}}}, \mathbf{h}_{\ell_{3\mathcal{I}}} = \hat{\mathbf{h}}_{\ell_{3\mathcal{I}}} \end{cases} \quad (19)$$

By substituting (19) into (12), UPEP $\mathcal{P}(\hat{\mathbf{a}}_i \rightarrow \hat{\mathbf{a}}_j)$ can be obtained, where the $\tilde{\psi}$ can be updated and rewritten as follows:

$$\tilde{\psi} = \frac{1}{2} \left(1 - \sqrt{\frac{\bar{\kappa}/2}{1 + \bar{\kappa}/2}}\right). \quad (20)$$

Finally, substituting (16), (19) and (20) into (12), we can rewrite the total probability of the error for HQAM-QSM scheme under the impact of imperfect channel knowledge as follows:

$$\tilde{\mathcal{P}}_e \approx \frac{1}{2^m} \sum_{i=1}^{2^m} \sum_{j=1}^{2^m} \frac{1}{m} \mathcal{P}_e(\hat{\mathbf{a}}_i \rightarrow \hat{\mathbf{a}}_j) e_{i,j}. \quad (21)$$

For the variable channel estimation error, when the channel estimation error is modeled as a function of SNR, i.e. $\sigma_\epsilon^2 = \frac{1}{\text{SNR}}$ where $\text{SNR} = \frac{E_s}{N_0}$, the approximate value of the asymptotic PEP expression can be written as follows [23]:

$$\begin{aligned} \mathcal{P}(\hat{\mathbf{a}}_i \rightarrow \hat{\mathbf{a}}_j) &= \frac{2^{3N_r-1} \Gamma(N_r + 0.5)}{\sqrt{\pi} (N_r)!} \left(\frac{1}{\text{SNR}}\right)^{N_r} \\ &\times \left[\frac{1 + 0.5 (|\mathcal{X}_{3\mathcal{R}}|^2 + |\hat{\mathcal{X}}_{3\mathcal{R}}|^2)}{\sigma_h^2 (|\mathcal{X}_{3\mathcal{R}}|^2 + |\hat{\mathcal{X}}_{3\mathcal{R}}|^2 + |\mathcal{X}_{3\mathcal{I}}|^2 + |\hat{\mathcal{X}}_{3\mathcal{I}}|^2)} \right]. \end{aligned} \quad (22)$$

4. Simulation results and discussion

In this section, computer simulation results are presented and compared in the presence of Rayleigh fading channels for HQAM-QSM, HQAM, traditional QSM, and SM with QAM techniques. The ML detector is used to estimate the transmitted symbols and indices. The SNR used in the simulations herein is defined as $\text{SNR}(\text{dB}) = 10 \log_{10}(E_s/N_0)$, where E_s is the average symbol energy. The rotation angle (ϕ) is counterclockwise.

The BER performances of the HQAM-QSM and TQAM-QSM schemes with $M = 4$ against the rotation angle (ϕ) are given in

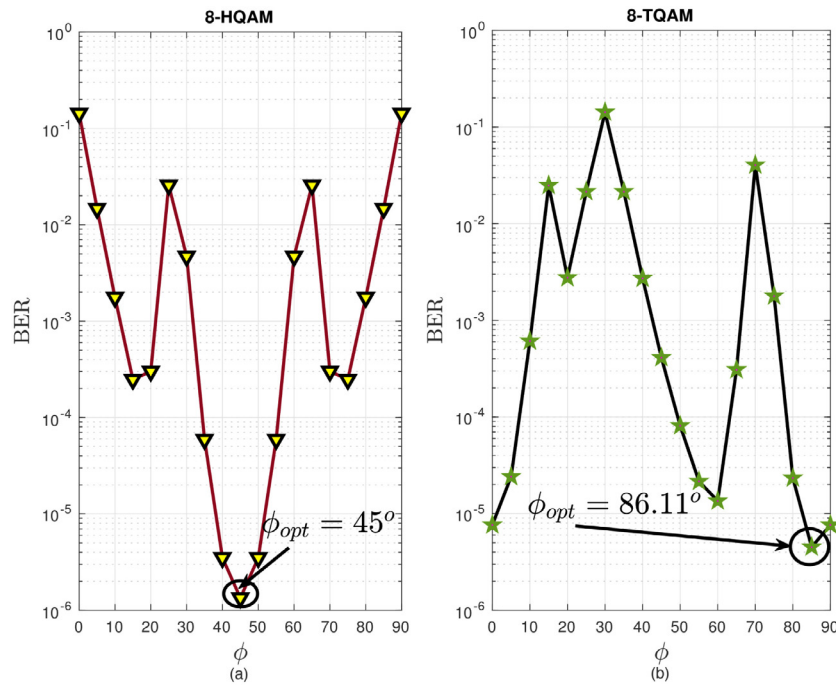


Fig. 6. BER vs. rotation angle of HQAM-QSM and TQAM-QSM scheme when $M = 8$ and SNR of 15 dB.

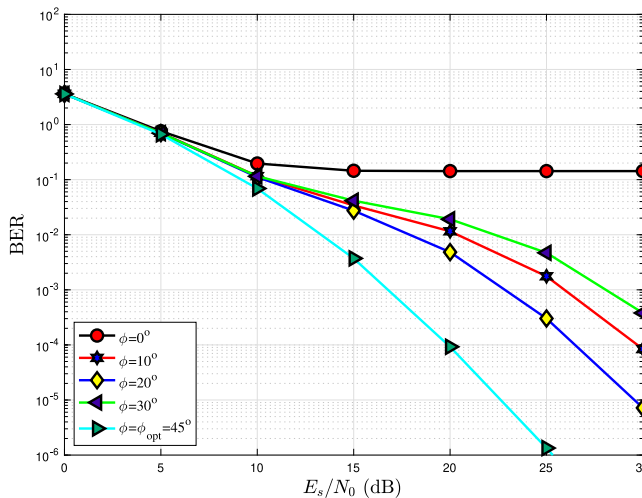


Fig. 7. Performance comparison curves of the HQAM-QSM technique when $\phi = 0^\circ, 10^\circ, 20^\circ, 30^\circ, 45^\circ$ and $N_T = N_R = 4$.

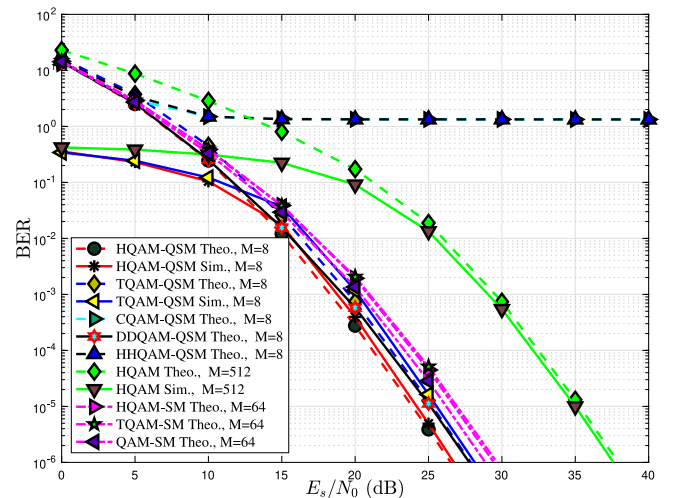


Fig. 8. Performance comparison curves for $m = 9$ bits/s/Hz when $N_T = 8, N_R = 4$.

Fig. 5 at the SNR of 15 dB when $N_T = N_R = 4$. As can be seen from Fig. 5, HQAM-QSM achieves the best BER value at an angle of 45 degrees, while the TQAM-QSM scheme achieves the best BER value at an angle of 75 degrees for the same M . In this case, $\phi_{opt} = 45^\circ$ for HQAM-QSM, and $\phi_{opt} = 75^\circ$ for TQAM-QSM.

In Fig. 6, the BER performance curves of the HQAM-QSM and TQAM-QSM schemes against the ϕ are depicted in Fig. 6 at the SNR of 15 dB when $N_T = N_R = 4$ and $M = 8$. As can be seen from Fig. 6, $\phi_{opt} = 45^\circ$ for HQAM-QSM, and $\phi_{opt} = 86.11^\circ$ for TQAM-QSM. As mentioned earlier, ϕ_{opt} changes completely due to the nature of constellation.

The BER performances of the HQAM-QSM technique with $N_T = N_R = 4$ are plotted in Fig. 7 when $\phi = 0^\circ, 10^\circ, 20^\circ, 30^\circ$ and, 45° . It can be seen from Fig. 7 and also Fig. 6a, when ϕ reaches ϕ_{opt} , error-floor disappears. As a result, HQAM-QSM achieves the

best BER value at an angle of 45 degrees and this angle is the optimum value (ϕ_{opt}) for $M = 8$.

In Fig. 8, BER performance curves of HQAM/TQAM/CQAM/DDQAM/HHQAM-QSM schemes with $N_T = 8$ and $M = 8$; conventional HQAM scheme with $M = 512$; HQAM-SM [16] and QAM-SM schemes with $N_T = 8$ and $M = 64$ for $N_R = 4$ bits are presented respectively. For a fair comparison, the number of transmitted bits for all schemes is selected as $m = 9$ bits/s/Hz. The best error performance from these hexagonal structures is HQAM-QSM (although the CFM value is lower than the DDQAM-QSM and HHQAM-QSM schemes) because the components of the constellation points have the best move-away from 0 points with a rotation of 45° . This feature also strengthens the compatibility of the HQAM-QSM structure, as mentioned earlier. As can be seen from the figure, CQAM-QSM and HHQAM-QSM schemes contain the (0, 0) point in them and cannot eliminate this point

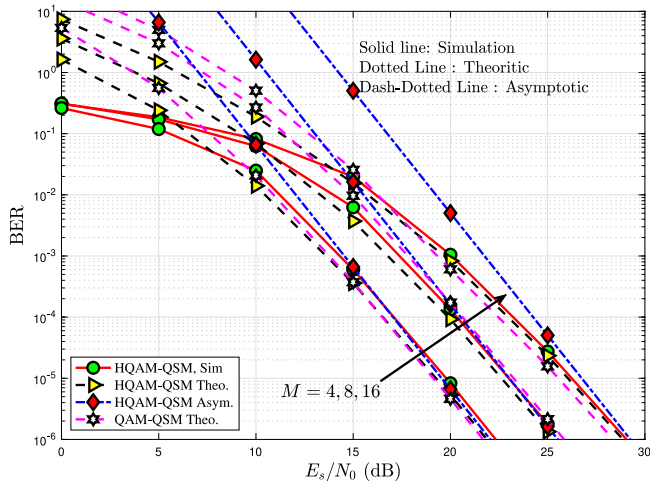


Fig. 9. BER curves of the proposed HQAM-QSM system for $N_T = N_R = 4$, $M = 4, 8$ and 16 .

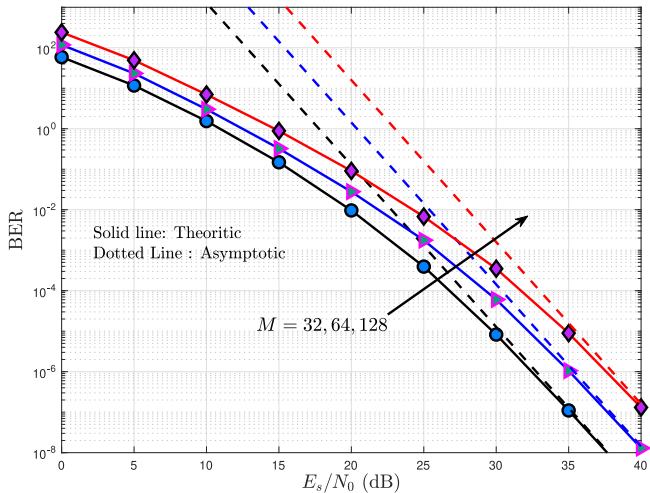


Fig. 10. BER curves of the proposed TQAM-QSM system for $N_T = 8, N_R = 4$, $M = 32, 64$ and 128 .

by rotation and result in the error-floor. It should be noted that the CQAM-QSM and HHQAM-QSM schemes give such a drawback in this modulation technique because of the structure of the QSM. Finally, we can see from Fig. 8 that our HQAM-QSM scheme has considerable SNR gains compared to conventional HQAM, HQAM-SM and QAM-SM techniques for the same number of bits per symbol.

Fig. 9 shows the BER performance curves of the HQAM-QSM method for $m = 6, 7$ and 8 bits when $N_T = N_R = 4$, and $M = 4, 8$ and 16 . For $M = 4$, the HQAM-QSM method transmits 4 bits of the $m = 6$ bits at the antenna index and 2 bits via the HQAM symbol; for $M = 8$, the HQAM-QSM method transmits 4 bits of the $m = 7$ bits at the antenna index and 3 bits via the HQAM symbol; for $M = 16$, the HQAM-QSM method transmits 4 bits of the $m = 8$ bits at the antenna index and 4 bits via the HQAM symbol. On the other hand, the BER performance curves of the TQAM-QSM method for $m = 11, 12$ and 13 bits when $N_T = 8, N_R = 4$, and $M = 32, 64$ and 128 are depicted in Fig. 10. For $M = 32, 64, 128$, the TQAM-QSM method transmits 6 bits at the antenna index and 5, 6, 7 bits via the TQAM symbol of the $m = 11, 12, 13$ bits, respectively. Also, the asymptotic PEP expressions given in (18) is illustrated in Figs. 9 and 10.

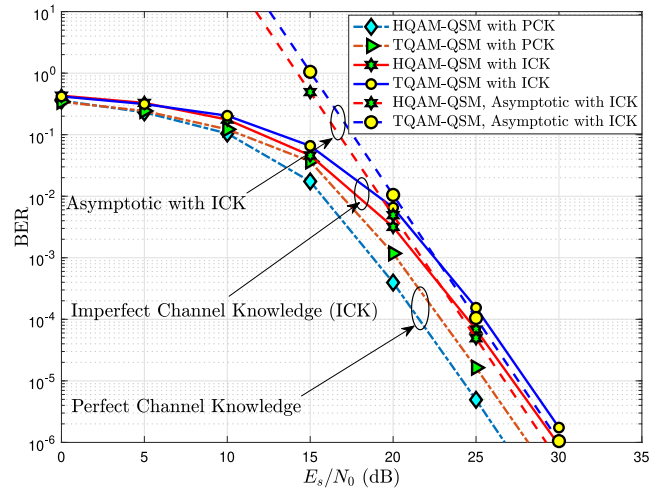


Fig. 11. BER curves of the proposed HQAM-QSM and TQAM-QSM system under the impact of imperfect channel knowledge for $N_T = 8, N_R = 4$, and $M = 8$.

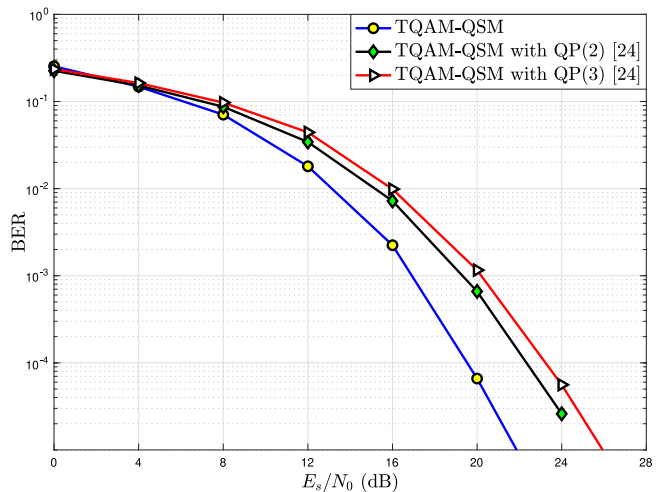


Fig. 12. BER curves of the proposed TQAM-QSM system under the suboptimal receiver for $N_T = N_R = 8$, and $M = 16$.

In Fig. 11, the impact of imperfect channel knowledge (ICK) on the performance of the proposed technique is examined. The channel estimation error is considered as $\sigma_\epsilon^2 = \frac{1}{\text{SNR}}$. BER performance curves of HQAM-QSM and TQAM-QSM schemes with $N_T = 8, N_R = 4$ and $M = 8$ are presented under the impact of ICK and perfect channel knowledge (PCK). Also, asymptotic BER performance curves of HQAM-QSM and TQAM-QSM schemes with ICK are presented. As can be seen from these BER curves, the obtained asymptotic curves with ICK are very close to the simulation results with PCK. The channel estimation error caused approximately 3 dB of performance loss for HQAM and 2.5 dB of performance loss for TQAM.

In Fig. 12, the performance curves obtained when using the low-complexity detector suggested in [25] instead of the ML detector at the receiver of the proposed system are presented. Here, each complexity represents a real multiplications. In the conventional QSM technique, the complexity is $\mathcal{O} = 8N_T^2MN_R$ when ML is used, while the total complexity is $\mathcal{O} = (8N_T^3 + 8N^2MN_R)$ when the less complex detector recommended in [25] is used at the receiver. Here, N indicates the degree of the quadratic programming (QP) technique and it is chosen as $N = 2, 3$

in Fig. 12. Under these conditions, the complexity of the TQAM-QSM system is $\mathcal{O}_{\text{TQAM-QSM}} = 65,536$ with ML, while $\mathcal{O}_{\text{TQAM-QSM}} = 4608$ and $\mathcal{O}_{\text{TQAM-QSM}} = 9728$ with [25] for $N = 2$ and $N = 3$, respectively. On the other hand, the ML-based TQAM-QSM system provides approximately 3 dB and 4 dB gain compared to QP(2) and QP(3) based TQAM-QSM systems, respectively.

5. Conclusions

In this study, a new HQAM aided QSM technique called HQAM-QSM is proposed, by combining HQAM and QSM techniques, for next-generation wireless communication systems with high data-rate and energy-efficiency. This proposed new system is inherently better in terms of energy-efficiency compared to traditional QSM with the QAM technique and is more advantageous in terms of symbol-separation at low energies. Due to the nature of HQAM symbols, error-floor occurs when the QSM system is applied. Hence, the optimum angle is obtained by rotating the HQAM symbols. With this optimum angle, it has been seen that the error-floor disappeared and the performance of the system is improved. Besides, the performance of the HQAM-QSM scheme has been analyzed thoroughly, the problems that may arise during the application of HQAM on the QSM system have been identified, and the solution methods of these problems have been explained in detail. Computer simulation results show that the proposed HQAM-QSM system provides similar error performance at high SNR values compared to the QSM with the QAM scheme while consuming less transmission energy.

CRedit authorship contribution statement

Fatih Cogen: Conceptualization, Visualization, Investigation, Software, Validation, Data curation, Writing - original draft, Writing - reviewing & editing. **Erdogan Aydin:** Methodology, Software, Validation, Supervision, Writing - original draft, Resources, Writing - reviewing & editing, Formal analysis.

Declaration of competing interest

The authors declare that they have no known competing financial interests or personal relationships that could have appeared to influence the work reported in this paper.

References

- [1] G.Y. Li, Z. Xu, C. Xiong, C. Yang, S. Zhang, Y. Chen, S. Xu, Energy-efficient wireless communications: Tutorial, survey, and open issues, *IEEE Wirel. Commun.* 18 (6) (2011) 28–35.
- [2] E. Aydin, F. Cogen, E. Basar, Code-index modulation aided quadrature spatial modulation for high-rate MIMO systems, *IEEE Trans. Veh. Technol.* 68 (10) (2019) 10257–10261.
- [3] N. Panwar, S. Sharma, A.K. Singh, A survey on 5G: The next generation of mobile communication, *Phys. Commun.* 18 (2016) 64–84.
- [4] L. Rugini, Symbol error probability of hexagonal QAM, *IEEE Commun. Lett.* 20 (8) (2016) 1523–1526.
- [5] C.D. Murphy, High-order optimum hexagonal constellations, in: 11th IEEE Int. Symp. on Pers. Indoor and Mobile Radio Commun. PIMRC 2000. Proceedings (Cat. No. 00TH8525), vol. 1, IEEE, 2000, pp. 143–146.
- [6] G. Xingxin, L. Mingquan, F. Zhenming, Asymmetric hexagonal QAM based OFDM system, in: IEEE 2002 Int. Conf. on Commun., Circuits and Systems and West Sino Expositions, vol. 1, IEEE, 2002, pp. 299–302.
- [7] P.K. Singya, P. Shaik, N. Kumar, V. Bhatia, M.-S. Alouini, A survey on design and performance of higher-order QAM constellations, 2020, arXiv: 2004.14708.
- [8] D. Sadhwani, R.N. Yadav, S. Aggarwal, D.K. Raghuvanshi, Simple and accurate SEP approximation of hexagonal-QAM in AWGN channel and its application in parametric α - μ , η - μ , κ - μ fading, and log-normal shadowing, *IET Commun.* 12 (12) (2018) 1454–1459.

- [9] D. Sadhwani, A. Agrawal, Performance analysis of hexagonal-QAM signals in Nakagami- m fading distribution, in: 2019 Int. Conf. on Signal Process. and Commun. (ICSC), 2019, pp. 82–85.
- [10] P. Singya, N. Kumar, V. Bhatia, M. Alouini, On performance of hexagonal, cross, and rectangular QAM for multi-relay systems, *IEEE Access* (ISSN: 2169-3536) 7 (2019) 60602–60616, <http://dx.doi.org/10.1109/ACCESS.2019.2915375>.
- [11] S. Stern, D. Rohweder, J. Freudenberger, R.F.H. Fischer, Binary multilevel coding over eisenstein integers for MIMO broadcast transmission, in: WSA 2019; 23rd Int. ITG Workshop on Smart Antennas, 2019, pp. 1–8.
- [12] P. Shaik, P.K. Singya, V. Bhatia, On impact of imperfect CSI over hexagonal QAM for TAS/MRC-MIMO cooperative relay network, *IEEE Commun. Lett.* (ISSN: 2373-7891) 23 (10) (2019) 1721–1724, <http://dx.doi.org/10.1109/LCOMM.2019.2931433>.
- [13] F. Cogen, E. Aydin, N. Kabaoglu, E. Basar, H. Ilhan, Code index modulation and spatial modulation: A new high rate and energy efficient scheme for MIMO systems, in: 2018 41st Int. Conf. on Telecommun. and Signal Process. (TSP). IEEE, 2018, pp. 1–4.
- [14] J. Jeganathan, A. Ghrayeb, L. Szczecinski, Spatial modulation: Optimal detection and performance analysis, 12, (8) 2008, pp. 545–547.
- [15] R.Y. Mesleh, H. Haas, S. Sinanovic, C.W. Ahn, S. Yun, Spatial modulation, *IEEE Trans. Veh. Technol.* 57 (4) (2008) 2228–2241.
- [16] F. Cogen, E. Aydin, Hexagonal quadrature amplitude modulation aided spatial modulation, in: 2019 11th Int. Conf. on Elect. and Electron. Eng. (ELECO), IEEE, 2019.
- [17] F. Cogen, E. Aydin, Performance analysis of HQAM based spatial modulation over nakagami- m fading channels, in: 2020 28th Signal Processing and Communications Applications Conference (SIU), 2020, pp. 1–4, <http://dx.doi.org/10.1109/SIU49456.2020.9302497>.
- [18] R. Mesleh, S.S. Ikki, H.M. Aggoune, Quadrature spatial modulation, *IEEE Trans. Veh. Technol.* 64 (6) (2015) 2738–2742.
- [19] S. Hosur, M.F. Mansour, J.C. Roh, Hexagonal constellations for small cell communication, in: 2013 IEEE Global Commun. Conf. (GLOBECOM), IEEE, 2013, pp. 3270–3275.
- [20] Z.Q. Taha, Construction of hexagonal-8-QAM constellation and code for OFDM, *Int. J. Enhanced Res. Sci. Technol. Eng. (IJERSTE)* 3 (3) (2014).
- [21] J. Ren, B. Liu, X. Xu, L. Zhang, Y. Mao, X. Wu, Y. Zhang, L. Jiang, X. Xin, A probabilistically shaped star-CAP-16/32 modulation based on constellation design with honeycomb-like decision regions, *Opt. Express* 27 (3) (2019) 2732–2746.
- [22] J. Ren, B. Liu, X. Wu, L. Zhang, Y. Mao, X. Xu, Y. Zhang, L. Jiang, J. Zhang, X. Xin, Three-dimensional probabilistically shaped CAP modulation based on constellation design using regular tetrahedron cells, *J. Lightwave Technol.* 38 (7) (2020) 1728–1734.
- [23] R. Mesleh, S.S. Ikki, On the impact of imperfect channel knowledge on the performance of quadrature spatial modulation, in: 2015 IEEE Wireless Communications and Networking Conference (WCNC), 2015, pp. 534–538.
- [24] M. Simon, M.S. Alaoui, *Digit. Commun. over Fading Channels*, John Wiley & Sons, New York, 2005.
- [25] Z. Yigit, E. Basar, Low-complexity detection of quadrature spatial modulation, *Electron. Lett.* 52 (20) (2016) 1729–1731, <http://dx.doi.org/10.1049/el.2016.1583>.



Fatih Cogen was born in Istanbul, Turkey. He received the B.S. degree of Computer Engineering (High Honors) and Electrical and Electronics Engineering (Double Major and High Honors) from Maltepe University; he graduated as the top-scoring student in the University. He received the M.S. degree of Electrical and Electronics Engineering from Istanbul Medeniyet University. He is currently pursuing his Ph.D. degree at Istanbul Medeniyet University and working as a research assistant at the Turkish-German University Mechatronics Engineering Department. His primary research interests include wireless communications, MIMO systems, cooperative communication and diversity, index Modulation, spatial modulation, two-way communication systems, and hexagonal constellations. He has authored or co-authored around seven papers in peer-reviewed journals and conferences. Fatih Cogen has served as a Reviewer of the IEEE Transactions on Vehicular Technology journal. Besides, he was awarded the best paper award in the field of telecommunications at the “2018 41st International Conference on Telecommunications and Signal Processing (TSP)” organized by IEEE.



Erdogan Aydin was born in Turkey. He received the B.S. with high honors and the M.S. degrees from Istanbul University, Istanbul, Turkey, in 2007 and 2010, respectively, and the Ph.D. degree from Yıldız Technical University, Istanbul, Turkey, in 2016. He is currently an Assistant Professor with the Department of Electronics and Communication Engineering, Istanbul Medeniyet University, Istanbul, Turkey. His primary research interests include MIMO systems, cooperative communication and diversity, reconfigurable intelligent

surfaces, index modulation, spatial modulation, media based modulation, hexagonal constellations, non-orthogonal multiple access, visible light communication, chaos communication, statistical signal processing, and estimation theory. He has received best paper award including one from the IEEE International Conference on Communications 2018. He has served as a TPC member for several IEEE conferences.

Dr. Aydin currently serves as a Review Editor of the *Frontiers in Communications and Networks*.